UCRL-96829
PREPRINT

COMPUTER MODELS FOR KINETIC EQUATIONS OF MAGNETICALLY CONFINED PLASMAS

J. Killeen
G. D. Kerbel
M. G. McCoy
A. A. Mirin
E. J. Horowitz
D. E. Shumaker

This paper was prepared for the Proceedings
of the
1987 International Conference
on Plasma Physics
Kiev, USSR

April 6-12, 1987

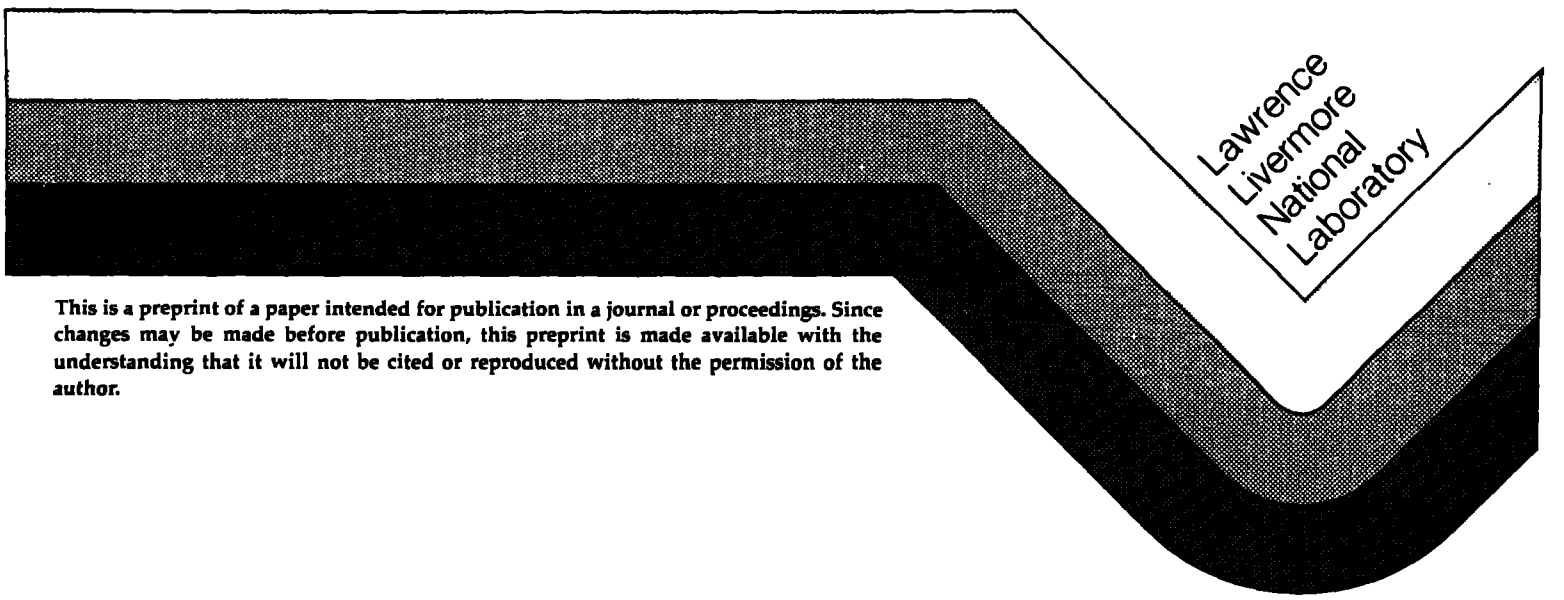

COMPUTER MODELS FOR KINETIC EQUATIONS OF MAGNETICALLY CONFINED PLASMAS*

J. Killeen, G.D. Kerbel, M.G. McCoy, A.A. Mirin
E.J. Horowitz, D.E. Shumaker

National Magnetic Fusion Energy Computer Center
Lawrence Livermore National Laboratory
University of California
Livermore, California

ABSTRACT

In this paper we present four working computer models developed by the computational physics group of the National Magnetic Fusion Energy Computer Center. All of the models employ a kinetic description of plasma species. Three of the models are collisional, i.e., they include the solution of the Fokker-planck equation in velocity space. The fourth model is collisionless and treats the plasma ions by a fully three-dimensional particle-in-cell method.

INTRODUCTION

During the early 1970's the U.S. magnetic fusion program supported at least fifteen varieties of experimental concepts. These were rather small experiments as compared to today's large facilities. During the years 1974 to 1980, the program went through a period of dramatic growth, but at the same time evaluations and reviews reduced the number of experimental concepts supported to the following;

Tokamak
Tandem Mirror
Reverse Field Pinch
Stellarator
Compact Toroids

The most advanced of the above concepts is the tokamak, and all four of the major international groups have commissioned large facilities

*Work performed under the auspices of the U.S. Department of Energy by the Lawrence Livermore National Laboratory under contract number W-7405-ENG-48.

to establish the scientific feasibility of fusion. All of the international groups are designing forms of "The Next Step," which is an ignition tokamak.

In all of these concepts, there are physics issues which must be addressed as a complete plasma system, i.e., they are interdependent. They include:

MHD Equilibrium and Stability
Perpendicular Ion and Electron Confinement
Parallel Confinement
Electric Potential
Heating
Fueling
Impurity Influx
Alpha Particle Heating

In order to resolve these issues, i.e., to reach a state where a fusion reactor is feasible, the experimental programs must be augmented by a program of computer modeling to aid in the design and interpretation of the experiments and implementation of theory. Because of the great variation in time and space scales[1] present in the plasma phenomena, relevant to the above fusion physics issues, the computational physicist develops computer models to address separate, more traditional, fusion theory questions. These include:

Vacuum magnetic surfaces
Ideal MHD equilibria
Stability
  Ideal MHD
  Resistive MHD
  Kinetic
Transport
  Neoclassical
  Anomalous

Heating
  Neutral Beams
  ICRH, ECRH, lower hybrid
  Alpha particles

The types of computer models that are developed include:

Time dependent macroscopic codes
  Fast time scale-resistive MHD
  Diffusion time scale-transport models
Time independent macroscopic codes
  Equilibrium
  Ideal MHD Stability
Vlasov and particle codes
Fokker-Planck codes
Hybrid codes

The term hybrid code describes the implementation of a model which treats some species of the plasma with a kinetic description in phase space and the remainder of the plasma species with a macroscopic (fluid) description.

Recent developments of these codes have emphasized the need for three dimensional models of the plasma phenomena. The implementation of these models requires the most advanced supercomputers available. The impact of new supercomputers on some of the types of models will be discussed later in this paper.

We present four working computer codes developed by the computational physics group of the National Magnetic Fusion Energy computer Center. Three of these codes are available to fusion researchers on the MFE Computer Network and the fourth one will be within a few months.

The MFE Computer Network (Figure 1) provides fusion researchers in the U.S. the full range of available computational power in the most

National MFE Network 1987

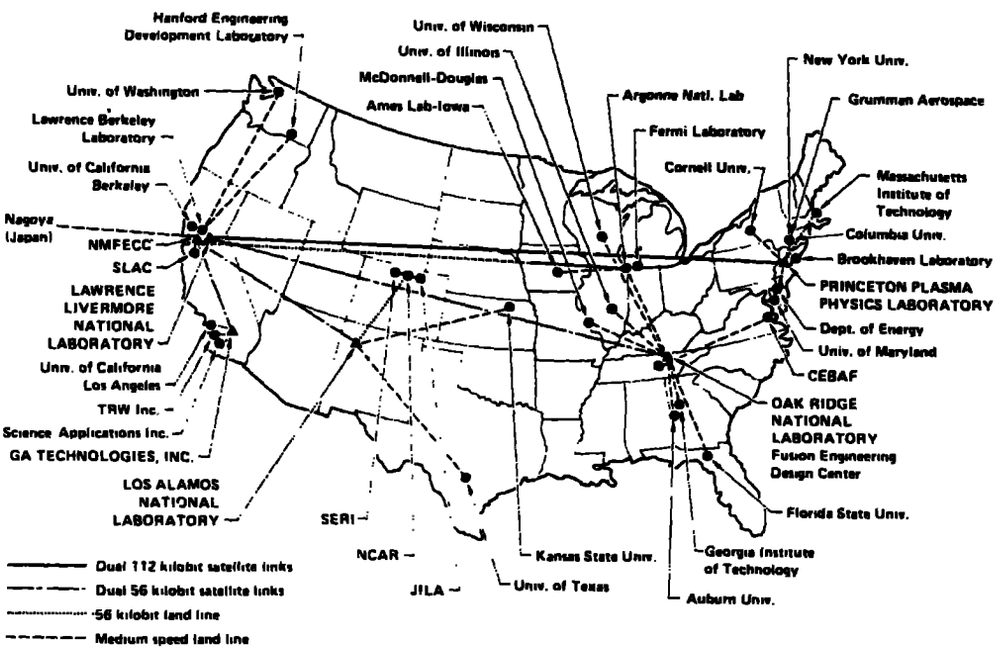

Figure 1

NMFECC hardware configuration

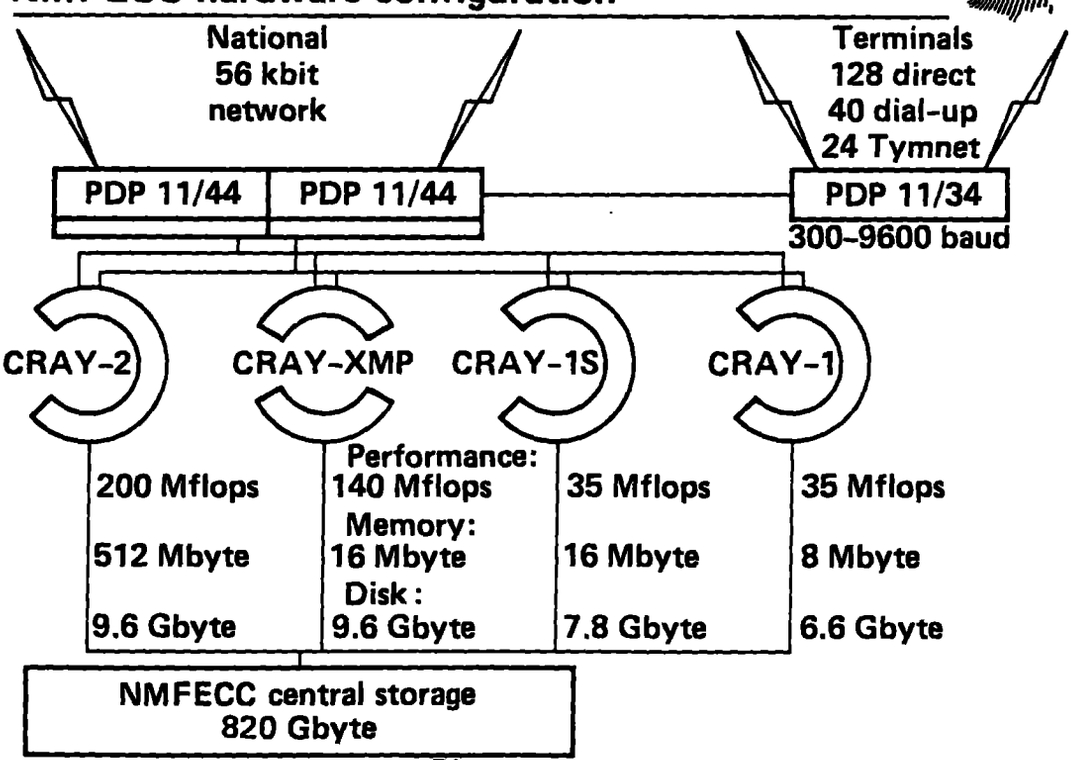

Figure 2

efficient and cost effective manner. This is achieved by using a network of computers of different capability tied together and to the users via dedicated data links and dial up telephone lines. The concept of the NMFECC is that different levels of computer capability are provided at the various locations according to research priorities. At the national center (Figure 2), providing high level capability to the entire community, are two high-speed Cray 1 computers, and a Cray X-MP/2. Additional equipment at the national center includes processors and other ADP equipment for communications, file management, and data storage. On May 28, 1985 the Serial 1 Cray 2 computer system was delivered to the NMFECC. This computer has four vector processors and 65 million words of MOS memory. This system gives the fusion community new capability required for advanced plasma modeling as described in the next sections.

COLLISIONAL KINETIC MODELS

Because magnetically confined plasmas are generally not found in a state of thermodynamic equilibrium they have been studied extensively with methods of applied kinetic theory.[2] In closed magnetic field line confinement devices such as the tokamak, non-Maxwellian distortions usually occur as a result of auxiliary heating and transport. In magnetic mirror configurations even the intended steady state plasma is far from local thermodynamic equilibrium because of losses along open magnetic field lines. In both of these major fusion devices, kinetic models based on the Boltzmann equation with Fokker-Planck collision terms have been successful in representing plasma behavior.[2,3] The heating of plasmas by energetic neutral beams[2,4] or microwaves,[2,5] the production and thermalization of α-particles in thermonuclear reactor plasmas, the study of runaway electrons in tokamaks, and the performance of two-energy component fusion reactors[2] are some examples of processes in which the solution of kinetic equations is appropriate and, moreover, generally necessary for an understanding of the plasma dynamics.

Ultimately, the problem is to solve a nonlinear partial differential equation for the distribution function of each charged plasma species in terms of six phase space variables and time. The dimensionality of the problem may be reduced through imposing certain symmetry conditions. For example, fewer spatial dimensions are needed if either the magnetic field is taken to be uniform or the magnetic field inhomogeneity enters principally through its variation along the direction of the field. Velocity dimensionality is reduced through phase averaging over the angular coordinates associated with nearly recurrent motion (e.g. gyromotion or bounce motion). Four independent variables--one spatial coordinate, two velocity space coordinates and time--are sufficient for many applications.

The development and implementation of the code "FPPAC"[2,6] a non-linear, two-dimensional multispecies, uniform-B, Fokker-Planck package has allowed its application to a large class of plasma kinetic theory problems. Through the recent development of the Fokker-Planck code "CQL"[2,5] it has become increasingly clear that non-uniform magnetic field effects ignored by "FPPAC" can play an essential role in determining plasma behavior. For instance, the electrical conductivity parallel to the magnetic field in a tokamak is strongly affected by the presence of a population of trapped electrons. Also cyclotron resonance heating and the production or support of steady plasma currents to allow steady state operation of tokamaks are significantly affected by the magnetic field non-uniformity.

The code "CQL" (for collisional, quasi-linear), like its precursor "FPPAC", is multispecies, 2-D and nonlinear. Unlike "FPPAC", however, the code is bounce-averaged and contains an RF quasilinear operator as an integral part of the Fokker-Planck time evolution model.[2,5] The consideration of these additional physical effects requires the analysis of a number of theoretical problems, the solutions to which provide the framework for the numerical mathematics utilized in "CQL". For instance, orbits which are nearly trapped but oppositely directed are topologically adjacent in velocity space and can populate each other through collisional

or resonant wave/particle diffusion. Internal jump conditions at the trapped/passing boundary are rigorously enforced by the numerical algorithm so as to maintain density conservation down to round-off.

The RF diffusion operator models lower-hybrid, multiple harmonic ICRH and ECRH scenarios. The evaluation of trajectory integrals for each gyro-orbit is done through the use of the stationary phase technique. This corresponds to performing the bounce-average of the wave/particle interaction operator. The collision operator can be bounce-averaged directly by numerical integration. By performing calculations on several flux surfaces in parallel (within the context of a new code constructed using "CQL" as a subroutine),[7] some very interesting radial coupling effects can be examined. In particular, with an additional dimension the issues surrounding wave propagation can be more readily addressed in a more consistent manner. A program[7] of this nature is ideally structured to exploit the power of the large memory, multi-tasking Cray-2 computer.

The modeling of neutral beam injection in tokamaks and the subsequent evolution of the fast ion distribution function requires the solution of Fokker-Planck equations. The first injection of neutral beams into tokamak plasmas took place at the Culham, Princeton, and Oak Ridge laboratories in 1972-73. The injected ions were studied with linearized Fokker-Planck models and the expected plasma heating was observed experimentally.

With the advent of much more powerful neutral beams, it became possible to consider neutral-beam-driven tokamak fusion reactors. For such devices, three operating regimes[8] can be considered: (1) the beam-driven thermonuclear reactor, (2) the two-energy component torus (TCT), and (3) the energetic-ion-reactor e.g. the counterstreaming ion torus (CBT). In order to study reactors in regimes (2) or (3), a nonlinear Fokker-Planck model must be used because most of the fusion energy is produced by beam-beam or beam-plasma reactions. Furthermore, when co and counter injection are used, or major radius compression is employed, a two

velocity-space dimensional Fokker-Planck operator is required.

Fortunately, the nonlinear, two-dimensional, multi-species Fokker-Planck model[2,3] had been developed for the mirror program. This model was applied successfully to several scenarios of TCT operation.[9,10] An important element of these simulations is the calculation of the energy multiplication factor, Q, for the various operating scenarios. This involves an accurate calculation of σv for each pair of reacting species. The methods developed for computing these multi-dimensional integrals are reported elsewhere.[11,12]

Neutral-beam-heated tokamaks are characterized by the presence of one or more energetic species which are quite non-Maxwellian, along with a warm Maxwellian bulk plasma. This background plasma may be described by a set of fluid equations. However, for cases in which there is a large energetic ion population, it is very important to represent the energetic species by means of velocity space distribution functions and to follow their evolution in time by integrating the Fokker-Planck equations. It is essential to utilize the full nonlinear Fokker-Planck operator to assure that the slowing down and scattering of these energetic species are computed accurately and realistically.

The successful application of the two-dimensional Fokker-Planck model to the energy multiplication studies of TCT led to the formulation of a more complete model of beam-driven tokamak behavior,[2,4] the Fokker-Planck/Transport (FPT) code. This model, in addition to solving one-dimensional radial transport equations for the bulk plasma densities and temperatures, solves nonlinear Fokker-Planck equations in two-dimensional velocity space for the energetic ion distribution functions, as a function of minor radius in the tokamak.

Fokker-Planck Equations

The appropriate kinetic equations are Boltzmann equations with Fokker-Planck Collision tems, often referred to simply as Fokker-Planck equations:

$$\frac{\partial f_a}{\partial t} + \underline{v} \cdot \frac{\partial f_a}{\partial \underline{r}} + \frac{\underline{F}}{m_a} \cdot \frac{\partial f_a}{\partial \underline{v}} = \left[\frac{\partial f_a}{\partial t}\right]_c + S_a + L_a \ . \qquad (1)$$

Here f_a is the distribution function in 6-dimensional phase space for particles of species a, S_a is a source term, $(\partial_a/\partial t)_c$ is the collision term, and L_a contains loss terms.

The Fokker-Planck collision term for an inverse-square force was derived by Rosenbluth, et al.[13] in the form

$$\frac{1}{\Gamma_a}\left(\frac{\partial f_a}{\partial t}\right)_c = -\frac{\partial}{\partial v_i}\left(f_a \frac{\partial h_a}{\partial v_i}\right) + \frac{1}{2}\frac{\partial^2}{\partial v_i \partial v_j}\left(f_a \frac{\partial^2 g_a}{\partial v_i \partial v_j}\right), \qquad (2)$$

where $\Gamma_a = 4\pi Z_a^4 e^4/m_a^2$. In the present work we write the "Rosenbluth potentials"

$$g_a = \sum_b \left(\frac{Z_b}{Z_a}\right)^2 \ell n\, \Lambda_{ab} \int f_b(\underline{v}')\,|\underline{v} - \underline{v}'|\, d\underline{v}' \ , \qquad (3)$$

$$h_a = \sum_b \frac{m_a + m_b}{m_b}\left(\frac{Z_b}{Z_a}\right)^2 \ell n\, \Lambda_{ab} \int f_b(\underline{v}')\,|\underline{v} - \underline{v}'|^{-1}\, d\underline{v}' \ , \qquad (4)$$

which differ from those given by Rosenbluth, et al.[13] in the dependence of the Coulomb logarithm on both interacting species and its consequent inclusion under the summations.

Since the collision term will be seen to contain velocity derivatives of f_a multiplied by velocity moments over f_a, Eq. (1) is a nonlinear, partial, integro-differential equation in 7 independent variables. We choose a spherical coordinate system for velocity space (with $\theta = 0$ corresponding to the direction along a magnetic field line) and a cylindrical coordinate system for physical space (z along the magnetic axis). With these coordinate systems, the following assumption is made:

The system is radially and azimuthally uniform in physical space, and hence, it is also azimuthally symmetric in velocity space. Equivalently, we neglect all gradients transverse to the magnetic field.

Eq. (2) in (v,θ) coordinates, written in conservation form is

$$\frac{1}{\Gamma_a}\left(\frac{\partial f_a}{\partial t}\right)_c = -\frac{1}{v^2}\frac{\partial G_a}{\partial v} + \frac{1}{v^2 \sin\theta}\frac{\partial H_a}{\partial \theta} , \tag{5}$$

where

$$G_a = A_a f_a + B_a \frac{\partial f_a}{\partial v} + C_a \frac{\partial f_a}{\partial \theta} \tag{6}$$

$$H_a = D_a f_a + E_a \frac{\partial f_a}{\partial v} + F_a \frac{\partial f_a}{\partial \theta} . \tag{7}$$

The coefficients A_a, B_a, C_a, D_a, E_a and F_a are given by:

$$A_a = \frac{v^2}{2}\frac{\partial^3 g_a}{\partial v^3} + v\frac{\partial^2 g_a}{\partial v^2} - \frac{\partial g_a}{\partial v} - v^2\frac{\partial h_a}{\partial v}$$

$$- \frac{1}{v}\frac{\partial^2 g_a}{\partial \theta^2} + \frac{1}{2}\frac{\partial^3 g_a}{\partial v \partial \theta^2} - \frac{\cot\theta}{v}\frac{\partial g_a}{\partial \theta} + \frac{\cot\theta}{2}\frac{\partial^2 g_a}{\partial v \partial \theta} \qquad (8)$$

$$B_a = \frac{v^2}{2}\frac{\partial^2 g_a}{\partial v^2} \qquad (9)$$

$$C_a = - \frac{1}{2v}\frac{\partial g_a}{\partial \theta} + \frac{1}{2}\frac{\partial^2 g_a}{\partial v \partial \theta} \qquad (10)$$

$$D_a = \frac{\sin\theta}{2v^2}\frac{\partial^3 g_a}{\partial \theta^3} + \frac{\sin\theta}{2}\frac{\partial^3 g_a}{\partial v^2 \partial \theta} + \frac{\sin\theta}{v}\frac{\partial^2 g_a}{\partial v \partial \theta}$$

$$- \frac{1}{2v^2\sin\theta}\frac{\partial g_a}{\partial \theta} + \frac{\cos\theta}{2v^2}\frac{\partial^2 g_a}{\partial \theta^2} - \sin\theta\frac{\partial h_a}{\partial \theta} \qquad (11)$$

$$E_a = \sin\theta\left[- \frac{1}{2v}\frac{\partial g_a}{\partial \theta} + \frac{1}{2}\frac{\partial^2 g_a}{\partial v \partial \theta}\right] \qquad (12)$$

$$F_a = \frac{\sin\theta}{2v^2}\frac{\partial^2 g_a}{\partial \theta^2} + \frac{\sin\theta}{2v}\frac{\partial g_a}{\partial v} \; . \qquad (13)$$

The system of equations given by Eq. (5) are solved by finite difference methods described in reference 2. The code "FPPAC" which implements this model has been published[6] in Computer Physics Communications.

The Fokker-Planck/Transport Code, FPT

The model presented here, in addition to solving one-dimensional radial transport equations for the bulk plasma densities and temperatures, solves nonlinear Fokker-Planck equations in two-dimensional velocity space for the energetic ion distribution functions. Moreover, neutral beam deposition and neutral transport are modeled using appended Monte Carlo codes developed elsewhere.[14,15]

An arbitrary number of energetic ion species are considered, whose presence derives from the ionization and charge exchange of injected fast neutrals. These species are described by distribution functions $f_b(v,\theta,r,t)$ in three-dimensional phase space, where b denotes the particle species, v is the velocity magnitude, θ is the pitch angle with respect to the magnetic field, and r is the distance from the magnetic axis.

The kinetic equation for the distribution function of energetic species b is

$$\frac{\partial f_b}{\partial t} = \left(\frac{\partial f_b}{\partial t}\right)_c + H_b - S_{bc} + S_{bcx} + \left(\frac{\partial f_b}{\partial t}\right)_E + \left(\frac{\partial f_b}{\partial t}\right)_r - L_b^{\alpha} - L_b^{orb} \quad . \tag{14}$$

The collision term $\left(\frac{\partial f_b}{\partial t}\right)_c$ is given by the complete nonlinear Fokker-Planck operator of Eq. (2). The quantity H_b is the source resulting from the injection of neutral species b.[14] S_{bc} represents the deceleration of energetic ions into the bulk plasma. S_{bcx} represents charge exchange between ion species b and the various neutral species. The quantity $\left(\frac{\partial f_b}{\partial t}\right)_E$ models the effect of the toroidal electric field. The term $\left(\frac{\partial f_b}{\partial t}\right)_r$

represents radial diffusion of the energetic ions. L_b^{α} is a fusion depletion term, and L_b^{orb} represents orbit losses. These terms are thoroughly described in reference 2.

An arbitrary number of bulk plasma ion species which are assumed to be Maxwellian in velocity space are considered. These species are described by densities $n_a(r,t)$ and by a common temperature profile $T_i(r,t)$. The electrons have a separately computed temperature profile $T_e(r,t)$, and their density is determined by quasineutrality; that is,

$$n_e = \sum_{\substack{\text{bulk} \\ \text{plasma}}} Z_a n_a + \sum_{\substack{\text{energetic} \\ \text{ions}}} Z_b n_b \quad . \tag{15}$$

Transport Equations

The ion densities and the ion and electron temperatures are described by the following set of equations:

$$\frac{\partial n_a}{\partial t} = -\frac{1}{r}\frac{\partial}{\partial r}\left(r\Gamma_a\right) + \int S_{bc}\,\underline{dv}\,\delta_{ab} + S_{ai} + S_{acx} - L_a^{\alpha} \tag{16}$$

$$\frac{\partial}{\partial t}\left(\frac{3}{2}\sum_a n_a T_i\right) = -\frac{1}{r}\frac{\partial}{\partial r}\left(r\sum_a Q_a\right) + \sum_{a,b}\int S_{bc}E_{bc}\,\underline{dv}\,\delta_{ab} + \sum_a S_{ai}\bar{E}_a + W_{cx} - \frac{3}{2}T_i\sum_a L_a^{\alpha} \tag{17}$$

$$+ \sum_{a,b} Q_{ab} + Q_{\Delta} + \sum_a Q_{a\alpha}$$

$$\frac{\partial}{\partial t}\left(\frac{3}{2}n_e T_e\right) = -\frac{1}{r}\frac{\partial}{\partial r}\left(rQ_e\right) + Q_{eb} - Q_{\Delta} + Q_{e\alpha} - \frac{3}{2}\frac{n_e T_e}{\tau_r} + j_{\phi}E_{\phi} \tag{18}$$

The quantities Γ_a, Q_a, and Q_e are particle and energy fluxes; E_{bc} is the mean energy of decelerated energetic ions; S_{ai} is the ionization source and $\bar{E}_a$ is the energy of neutral species "a"; S_{acx} and W_{cx} describe charge exchange; L_a^{α} represents fusion depletion; Q_{ab} models heating by the energetic species; Q_{Δ} is energy exchange between bulk ions and electrons; $Q_{a\alpha}$ is alpha particle heating; τ_r is the radiation loss time; and $j_{\phi}E_{\phi}$ represents Ohmic heating. The particle and energy fluxes are written as linear combinations of the density and temperature gradients and of the toroidal electric field. This makes possible the representation of a full multispecies neoclassical transport model, as described by Mirin, et al.[16] However, present-day tokamaks do not generally obey neoclassical scaling laws;[17] hence, empirical transport models are often employed.

The boundary conditions are rather straight-forward. At the limiter, small values of n_a, T_e and T_i are imposed. At $r = 0$ conservation boundary conditions are employed. That is, Eq's. (16) - (17) are used but with flux derivatives $-\frac{1}{r}\frac{\partial}{\partial r}(rF)$ replaced by $-2F/_r$ evaluated one-half meshpoint from $r = 0$. With the proper numerical integration scheme, the total number of ions and the total ion and electron energies are properly conserved (modulo known source and loss terms). The resulting system of difference equations is block tridiagonal, and it is solved using standard methodology.[18]

There are three contributions to the fusion reaction rate: (i) thermonuclear reactions, denoted R_{11}; (ii) "beam-target" reactions, denoted R_{12}; and (iii) reactions among the energetic ions, denoted R_{22}. At each plasma radius, the fusion reactivities $\langle\sigma v\rangle_{11}$, $\langle\sigma v\rangle_{12}$ and $\langle\sigma v\rangle_{22}$ are evaluated numerically via a five-fold velocity-space integral[11,12]

$$R_{ij} = \int f_i(\underline{v}_i)\, f_j(\underline{v}_j)\, \sigma\,(\underline{v}_i - \underline{v}_j)\, |\underline{v}_i - \underline{v}_j| \underline{dv}_i \underline{dv}_j \quad . \qquad (19)$$

The R_{ij} are then integrated over the plasma volume, to give the total reaction rate.

Recent Applications of FPT

The code was used to simulate neutral beam injection in the Tokamak Fusion Test Reactor (TFTR) at low to moderate density.[19] In the simulation the transport mechanisms are turned off, and the measured profiles of n_e and T_e and an estimated one for T_i are specified and a neutral density is assumed. The Fokker-Planck equations for the energetic ions are iterated to steady-state solutions using the experimental plasma parameters and profiles for the target plasma.

There is considerable uncertainty concerning Z_{eff} in the central plasma region and the radial profile of impurity concentration. For the low $\bar{n}_e$-low current conditions studied in Table 1, measurements indicate that $Z_{eff} \gtrsim 2.0$. Table I gives the results of FPT calculations for different values of Z_{eff} (here assumed to be independent of radius). The quantity which is compared to the experimental measurements is S, defined as the instantaneous fusion neutron production rate in neutrons/second. Here

$$S = S_{bb} + S_{bt} + S_{tt} \tag{20}$$

where S_{bb} are beam-beam neutrons, S_{bt} are beam-target neutrons, and S_{tt} are thermonuclear neutrons. It turns out that for purely co-injected beams, as in the present experiments, the predicted S is only weakly dependent on Z_{eff}. When $Z_{eff} = 1$, there is little pitch-angle scattering of the energetic ions, and 12% of S is due to beam-beam reactions. When Z_{eff} increases, S_{bt} is reduced by impurity dilution of the target-ion population. (The decrease in n_h/n_e is due to the electrons that neutralize the impurity ions.) On the other hand, at $Z_{eff} = 4$, pitch-angle scattering of the energetic ions is enhanced, thereby increasing $\langle \sigma v \rangle_{bb}$ so that S_{bb} accounts for 44% of the total reaction rate. The increase in S_{bb} compensates for the decrease in S_{bt}.

In both cases, n_h/n_e in the plasma center is calculated to be close to 0.6, although when averaged over the plasma volume, $\langle n_h/n_e \rangle \approx 0.17$. The results in Table I also show that if one of the two beams were to be counter-injected rather than co-injected, the neutron source strength would be even higher, the exact amount depending on Z_{eff}. This increase comes from the greatly enhanced beam-beam reactivity $\langle \sigma v \rangle_{bb}$ in the CBT mode,[8] as well as the elimination of plasma rotation by the balanced beam injection. These effects have imnportant influence on S only at low plasma density. The higher S values expected from balanced injection for beam-beam reactions would also be much less pronouned in future D-T experiments with E_b = 120 keV, due to the D-T reactivity maximum at about 125 keV relative energy.

Additional FPT analyses indicate that a relatively small increase in density (a factor ≃ 1.5) causes the plasma to switch over to a regime where n_h/n_e at r = 0 is reduced to about 0.2. In this case more than half the fusion reactivity comes from beam-target reactions and most of the rest from thermonuclear reactions.

TABLE I. FPT Code Calculation of Sources of Fusion Neutrons at Low Density[a]

		Results of FPT Calculations[b]				
			TOTAL	% Distribution of Reactions		
Injector Orientation	Z_{eff}	n_h/n_e at r=0	S 10^{14}/s	BEAM-BEAM	BEAM TARGET	THERMAL IONS
Co-injectn. only	1.0	0.62	7.7	12	74	14
"	1.5	0.61	7.2	20	68	12
"	4.0	0.49	5.6	44	51	5
1 Co-inj. & 1 ctr-inj.	1.0	0.64	11.4	41	49	10
"	1.5	0.58	9.9	43	48	9
	4.0	0.47	6.8	54	41	5

[a]Experimental conditions: coinjection only; $T_e(0)$=4.2 keV; I_p=0.8 MA; P_b=4.8 MW; $n_e(0)=2.2\times10^{19}$ m^{-3}; measured S=3.3×10^{14} n/s, E_b=80 keV

[b]Plasma rotation not included.

The results shown in Table II were calculated using experimental conditions for low density TFTR shots that gave approximately 3.3 x 10^{14} n/s for D→D. The warm ions are represented as displaced Maxwellians, with the rotation speed assumed to be parabolic in radius. Evidently, the large plasma rotation observed at low $\bar{n}_e$ is found to cause a significant reduction in the calculated beam-target reaction rate. The beam-target source strength drops by 54% with rotation when Z_{eff} = 1.0, by 49% when Z_{eff} = 1.5 and by 35% when Z_{eff} = 4. In the latter cases pitch-angle scattering of the hot (beam-injected) ions is enhanced, so that velocity displacement of the warm ions has much less effect on the average relative velocity of the hot and warm ions.

In the results shown in Table II, bulk ion rotation was included both in calculating the beam-target reactivity $\langle\sigma v\rangle_{bt}$ and in the Fokker-Planck operator. Rotation of the bulk plasma causes the co-injected fast ions to thermalize more quickly, because of the reduced relative velocity with the thermal ions. However, the dominant effect on S resulting from plasma rotation is due to the change in the beam-target reactivity.

Table II. FPT Code Calculation of Effect of Bulk-Plasma Rotation on Neutron Source Strength[a,b]

		Results of FPT Calculation			
	Central		Neutron Source Strength(10^{14}n/s)		
Z_{eff}	Rotation (keV)	TOTAL S	BEAM-BEAM	BEAM-TARGET	THERMAL IONS
1.0	0.0	7.7	1.0	5.7	1.0
1.0	5.0	4.3	0.6	2.6	1.1
1.5	0.0	7.2	1.5	4.9	0.9
1.5	5.0	4.5	1.1	2.5	0.9
4.0	0.0	5.6	2.4	2.9	0.3
4.0	5.0	4.5	2.3	1.9	0.3

[a] A rotation of 5.0 keV corresponds to 7x10^5 m/s for deuterons.
[b] Experimental conditions: coinjection only; $T_e(0)$=4.2 keV; I_p=0.8 MA; P_b=4.8 MW; $n_e(0)$=2.2x10^{19} m^{-3}; Measured S=3.3x10^{14}n/s.E_b=80 keV

The planned increase in beam voltage to 120 kV, with greatly improved beam species composition, is expected to increase Q by a factor of about 3 based on the energy dependence of $\langle\sigma v\rangle_{bt}$ and τ_s, for the same bulk-plasma parameters. Of the four beam injectors now installed, one is oriented for counter-injection; the increase in energetic-ion reactions at low density should lead to another factor of at least 1.5 increase in S_{bb}, for the same beam power and bulk-plasma conditions. Thus overall Q will increase by a factor of approximately 5, reaching about 5×10^{-4} in deuterium only. (Figure 3) The importance of beam-beam reactions at low density can be seen in Figure 4. FPT code simulations shown that $n_h \simeq n_e$ for $r \lesssim 30$ cm.

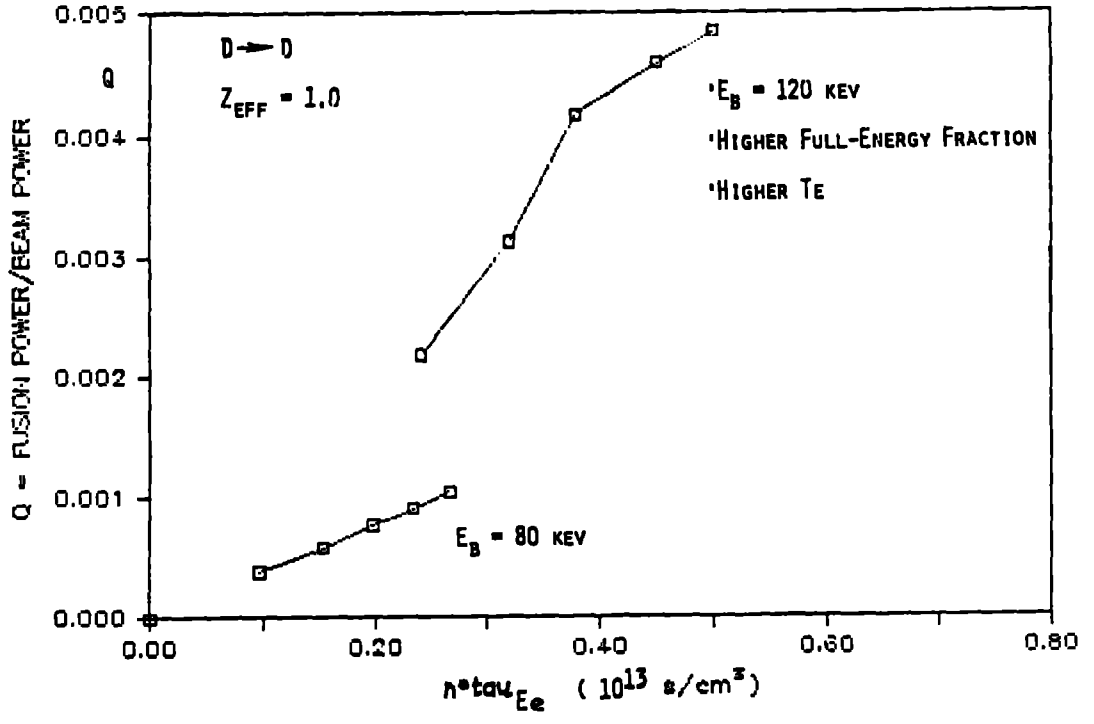

Figure 3

FPT calculations of Q vs n τ_{Ee}. For 80-kev beams with present species mix (≈50% power at full energy), and 120-kev beams with improved species mix (67% power at full energy).

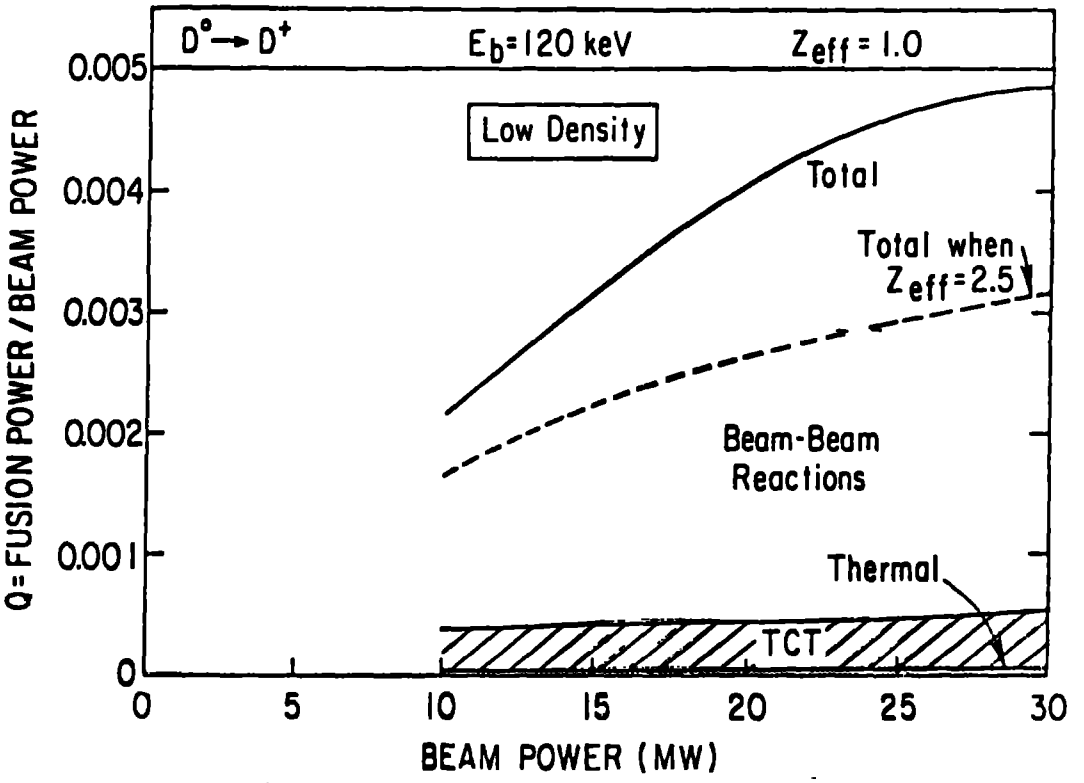

Figure 4

FPT simulations of TFTR performance in D-D with improved-species, 120-kev beam injectors, in a low-density regime dominated by beam-beam reactions. Simulations with D & T beam injection indicate that $Q \approx 1$ can be attained if $Z_{eff} \approx 1$.

The Fokker-Planck simulations show (Figure 5) that only a relatively small increase (factor - 1.5) in plasma density is required to switch the principal source of fusion-neutron production from beam-beam and beam-target reactions, to beam-target and thermonuclear reactions, with relatively small changes in Q at the transition. Further simulations indicate that this feature will persist as the injected power is raised to the 30 MW level, and E_b increases to 120 keV with improved beam species composition. Thus the choice of operating regime may depend on the level of τ_{Ee} that can be attained, and in the case of D-T operation, whether tritium beams are available.

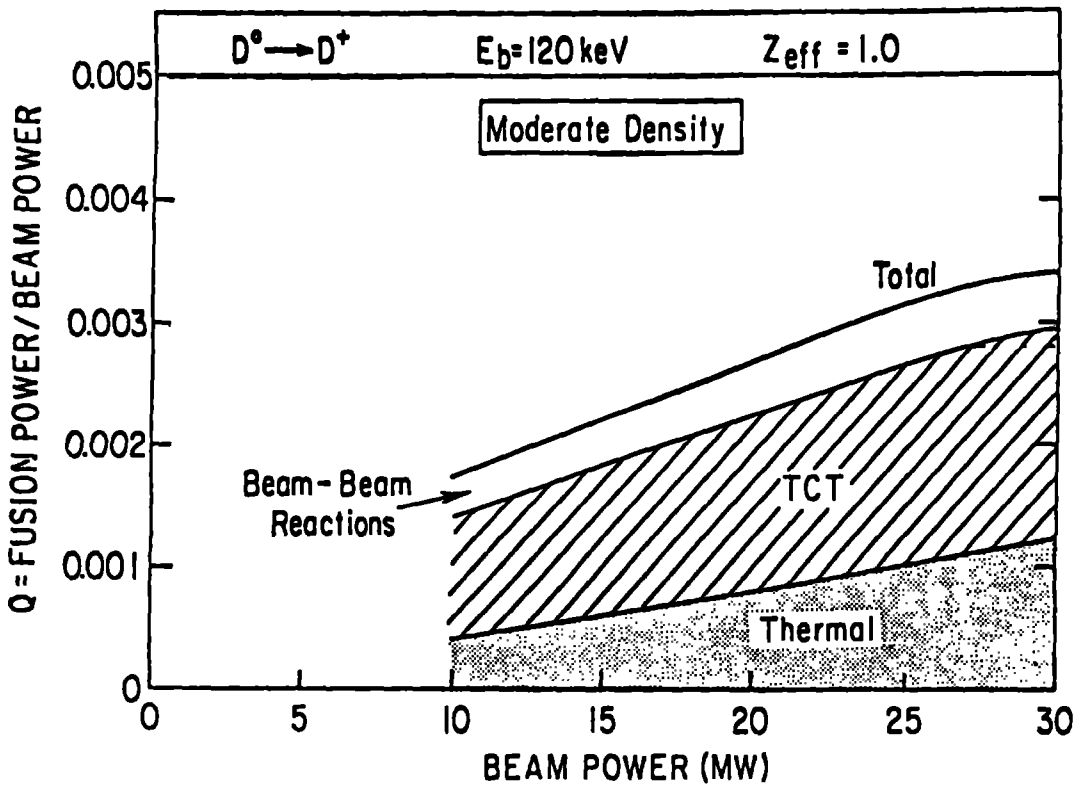

Figure 5

FPT simulations of TFTR performance in D–D with improved-species, 120-kev beam injectors, in a moderate-density regime dominated by beam-target (TCT) reactions. Simulations with a tritium target plasma indicate that $Q \approx 1$ can be attained if $Z_{eff} \approx 1$.

COLLISIONLESS KINETIC MODELS

In many cases fluid models are not adequate to describe plasma behavior, for it is necessary to consider microscopic effects, i.e., the effects of the way particles are distributed in velocity. Numerically this is most often accomplished through particle codes.[20-22] Fully nonlinear kinetic ion and electron simulations in 2-D Cartesian geometry have been carried out over the last decade. In the past, Cartesian geometry was not a major physics limitation even with the obvious cylindrical and toroidal nature of experiments, because these models necessarily dealt with length and time scales on the order of the electron gyroradius and plasma oscillation period for stability. Resolving such length and time scales meant that any realistic macroscopic dimension could be considered infinite. With

the increase of grid resolution allowed by improved computers and methodology, the scope of particle simulations has grown to encompass nonlocal effects and more realistic geometries.

On the Cray-1 computers, large scale particle simulations in 2-1/2D and 3D are mainly limited by the size of the maximum fast memory. Experimentally relevant physics problems in magnetic confinement have important three-dimensional aspects, and the Cray-2 with its four vector processors and large memory makes realistic 3D simulations feasible.

Particle-fluid hybrid models have become important in the last five years.[23-24] A typical hybrid model represents the ion components as kinetic species and the electrons as a fluid in order to eliminate some or all fast electron frequencies and short length scales. Recent progress with hybrid models is impressive, but the capabilities of the Cray-2 are clearly needed for three-dimensional models.

A three-dimensional model, QN3D, has been developed at the NMFECC using a particle model for ions and an inertialess fluid model for electrons. The code is designed to use the capabilities of the Cray-2, taking advantage of the large memory and multi-tasking as well as the ability to vectorize gather and scatter operations. The latter is important when interpolating particle quantities to the grid (Fig. 6) and vice versa.[25] A method of sorting the particles to allow vectorization of the collections of charges and currents onto the grid is used with an overall reduction in CPU time of about 50% over scalar coding. The particles are advanced using a leap-frog scheme and the fields are solved on a grid using a Darwin[22] model and quasi-neutrality.

The equations for the electromagnetic fields, the electron current and the ion motion are

$$\nabla \times \bar{E} = \frac{1}{c}\frac{\partial \bar{B}}{\partial t} \tag{21}$$

$$\nabla \times \bar{B} = \frac{4\pi}{c}\bar{J} \tag{22}$$

$$\bar{E} = \frac{\bar{J}_e \times \bar{B}}{en_i c} \tag{23}$$

$$M\frac{d\bar{v}_i}{dt} = e\bar{E} + \frac{e}{c}\bar{v}_i \times \bar{B}_i \tag{24}$$

where $\bar{J}_e = -en_i\bar{U}_e$. Notice that we have set $n_e = n_i$ consistent with quasineutrality.

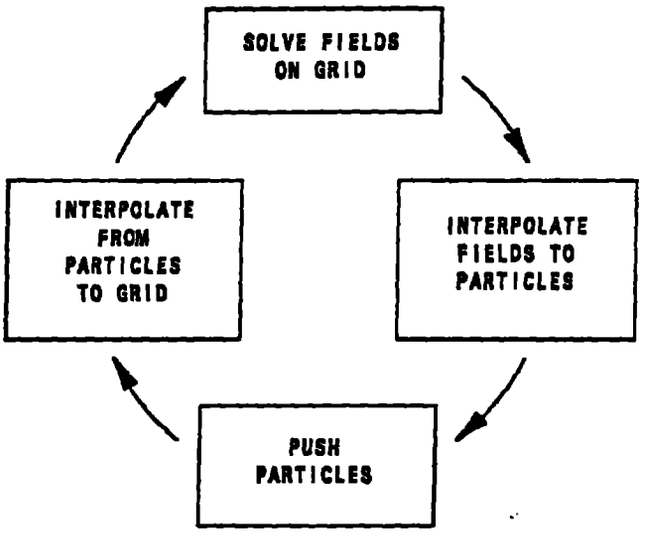

Figure 6
The Computational Cycle

The code starts with fields given on the grid at time step 0, particle positions given at time step 0 and particle velocities given at time step -1/2. The cycle starts with interpolating fields to the particle positions.

The code, QN3D, has been verified with several test problems, in particular single particle motion, normal mode propagation, and the rigid rotor instability.[26]

The code is used to model the tilt mode in Field Reversed Configurations (FRCs). This mode is unusual in that MHD codes have predicted violent growth but experiments have seen no growth at all. We believe that the finite ion orbits which are ignored by MHD codes provide the essential

stabilization. If this is the case, then larger experiments might see the tilt mode as the ion orbits become less significant in relation to the other relative length scales.

For this application, QN3D is given an initial equilibrium from EQV, a 2-D (r-z) Vlasov equilibrium code. This equilibrium code assumes that the ion distribution is a given function of the Hamiltonian and the canonical angular momentum and the electrons are modeled as a cold, inertialess fluid as in QN3D.

As mentioned above, we expect the tilt mode to be unstable when the ion gyroradius becomes small with respect to the size of the plasma. A convenient measure of this relative size is s, which, itself, is a measure of the number of ion gyroradii between the o-point and separatrix. For higher s we would expect the plasma to act like a fluid. We define s as

$$s = \int_R^{r_s} \frac{r}{r_s} \frac{dr}{\rho_i(r)}, \tag{25}$$

where R is the o-point radius, r_s is the separatrix radius and ρ_i is the ion gyroradius. We investigated two cases, one with s = 1.6 and another with s = 12. The parameters of these runs are summarized in table III.

	s = 12	s = 1.6
Background $\bar{B}$	2.2×10^4 G	2.7×10^3 G
Peak Density	$7.0 \times 10^{16}/cm^3$	$1.1 \times 10^{15}/cm^3$
Alfvén Speed	1.82×10^7cm/s	1.78×10^7cm/s
Ion Temperature	200 eV	200 eV
MHD Growth Time	0.97 μs	0.99 μs
Computed Growth Time,ON3D.	0.92 μs	12.6 μs

Both cases used 1,000,000 particles in a grid 41 cubed

Table III: Tilt Mode Parameters

We used many diagnostics to observe the tilt mode. First, we plotted flux contours. For a cylindrically symmetric configuration the flux contours are also contours of constant ψ where

$$\psi = rA_\theta .$$

and we find A_θ by solving

$$-\nabla^2 \vec{A} = \frac{4\pi}{c}\vec{J}$$

This was very helpful in that we were able to see the plasma tilting very easily in the high-s case and not at all in the low-s case. However, when the plasma starts to tilt, it loses its axisymmetry and the contours of constant ψ are no longer the flux surfaces of the magnetic field. Nevertheless, these plots gave us a qualitative indication that the phenomena was occuring in the high-s regime and not in the low-s regime (see figures 7 & 8).

It is important to remember that the tilt mode instability observed here grew out of the noise in the simulation introduced by the random nature of the particle initialization. No initial perturbation was employed to help the plasma develop the tilt.

We have been able to give strong credence to our initial hypothesis that the tilt mode will exist in regimes of higher s. This result, by itself, is important for those planning to build larger FRC experiments. But, in addition, QN3D has a major advantage in that it is able to model the nonlinear regime of the tilt mode which will be even more crucial to the future of FRC experiments.

It is worthwhile to note that the computations presented here would have been impossible without the Cray-2 computer. The field length of QN3D for these runs was about 25 million words (which isequivalent to 1.6 trillion bits).

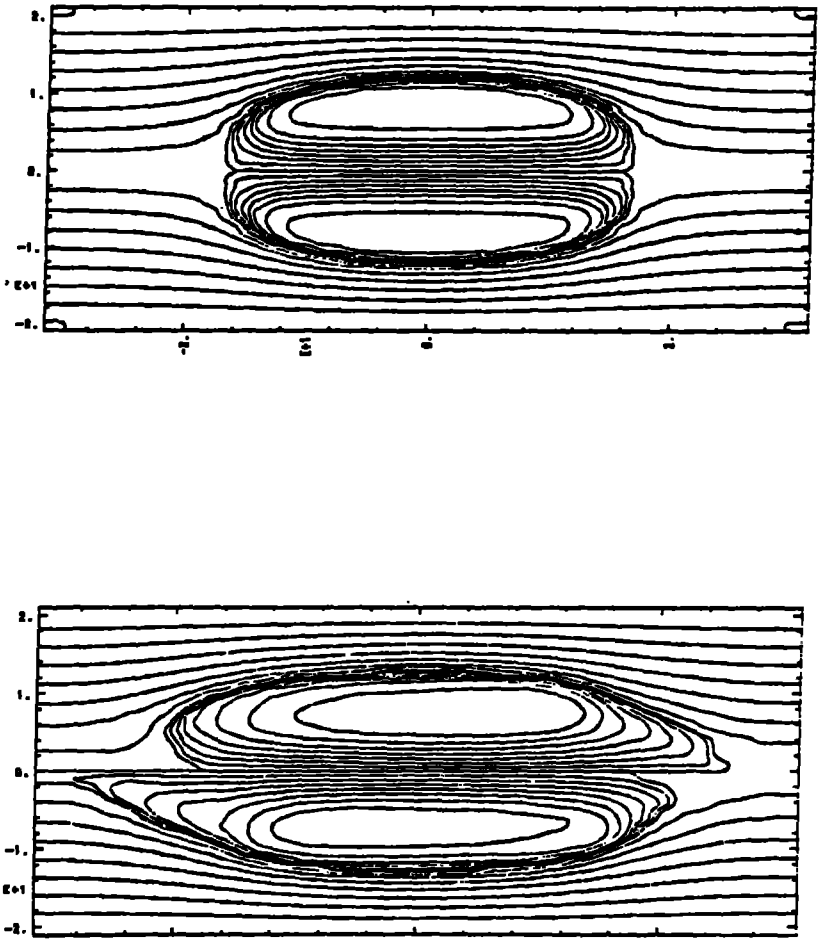

Top: 0μs Bottom: 2μs

Figure 7

Tilting ψ Surfaces: s = 12

REFERENCES

1. Cohen, B.I. and Killeen, J., Computations in Plasma Physics, Physics Today (May 1983), 54-63.

2. Killeen, J., Kerbel, G.D., McCoy, M.G., and Mirin, A.A., Computational Methods for Kinetic Models of Magnetically Confined Plasmas, Springer Series in Computational Physics (Springer-Verlag, New York, 1986).

3. Killeen, J., Mirin, A.A., and Rensink, M.E., The Solution of the Kinetic Equations for a Multispecies Plasma, in: Killeen, J. (ed.), Methods in Computational Physics, Vol. 16 (Academic Press, New York, 1976), 389-431.

4. Killeen, J., Mirin, A.A., and McCoy, M.G., A Fokker-Planck/Transport Model for Neutral Beam Driven Tokamaks, in: McNamara, B. (ed.), Modern Plasma Physics (IAEA, Vienna, 1981), 395-416.

5. Kerbel, G.D. and McCoy, M.G., Kinetic Theory and Simulation of Multi-Species Plasmas in Tokamaks Excited with ICRF Microwaves, Phys. Fluids 28 (1986), 3629-3653.

6. McCoy, M.G., Mirin, A.A., and Killeen, J., FFPAC - A Two-Dimensional Multi-Species Nonlinear Fokker-Planck Package, Comp. Phys. Commun. 24 (1981), 37-61.

7. McCoy, M.G., Kerbel, G.D., and Harvey, R.W., Three-dimensional Simulations of Radio Frequency Heating, Bull. Am. Phys. Soc. II 30 (1985), 1591.

8. Jassby, D.L., Nucl. Fusion 17 (1977), 3009.

9. Killeen, J., Johnson, T.H., Mirin, A.A., and Rensink, M.E., "Computational Studies of the Two-Component Toroidal Fusion Test Reactor," Report UCID-16530, Lawrence Livermore National Laboratory, Livermore, CA (1974).

10. Killeen, J., Marx, K.D., Mirin, A.A., and Rensink, M.E., Proc. 7th Europ. Conf. Controlled Fusion and Plasma Physics, Lausanne, 1975 1 (1975), 22.

11. Marx, K.D., Mirin, A.A., McCoy, M.G., Rensink, M.E., and Killeen, J., Nucl. Fusion 16 (1976), 702.

12. Cordey, J.G., Marx, K.D., McCoy, M.G., Mirin, A.A., and Rensink, M.E., J. Comp. Phys. 28 (1978), 115.

13. Rosenbluth, M.N., MacDonald, W.M., and Judd, D.L., Phys. Rev. 107 (1957), 1.

14. Lister, G.G., Post, D.E., Goldston, R., Plasma Heating in Toroidal Devices (Varenna, Italy), 303 (1976).

15. Hughes, M.H. and Post, D.E., J. Comp. Phys. 28 (1978), 43.

16. Mirin, A.A., Killeen, J., Marx, K.D., and Rensink, M.E., J. Comp. Phys. 23 (1977), 23.

17. Furth, H.P., Nucl. Fus. 15 (1975), 487.

18. Richtmyer, R.D. and Morton, K.W., Difference Methods for Initial-Value Problems (Interscience, New York), Second Edition (1967).

19. Hendel, H.W., England, A.C., Jassby, D.L., Mirin, A.A., and Nieschmidt, E.B. Fusion-Neutron Production in the TFTR with Deuterium Neutral-Beam Injection, J. of Fusion Energy, 5 (1986), 231-244.

20. Dawson, J.M., Okuda, H., and Rosen, B., Collective Transport in Plasmas, in: Killeen, J. (ed.), Methods in Computational Physics, Vol. 16 (Academic Press, New York, 1976), 282-326.

21. Langdon, A.B. and Lasinski, B.F., Electromagnetic and Relativistic Plasma Simulation Models, in: Killeen, J. (ed.), Methods in Computational Physics, Vol. 16 (Academic Press, New York, 1976), 327-366.

22. Nielson, C.W. and Lewis, H.R., Particle-Code Models in the Nonradiative Limit, in: Killeen, J. (ed.), Methods in Computational Physics, Vol. 16 (Academic Press, New York, 1976), 367-388.

23. Hewett, D.W., A Global Method of Solving the Electron-Field Equations in a Zero-Inertia-Electron-Hybrid Plasma Simulation Code, J. Comput. Phys. 38 (1980), 378-395.

24. Harned, D.S., Quasineutral Hybrid Simulation of Macroscopic Plasma Phenomena, J. Comput. Phys. 47 (1982), 452-462.

25. Horowitz, E.J., Vectorizing the Interpolation Routines of Particle-in-Cell Codes, J. Comput. Phys. 68 (1987), 56-65.

26. Harned, D.S., Rotational Instabilities in the Field-Reversed Configuration: Results of Hybrid Simulations, Phys. Fluids 26 (1983), 1320-1326.